ENTICE Satellite Orbital Simulator to Study Ice Clouds

Kyle Johnson[1], Jonathan H. Jiang[2,*], Qing Yue[2], Kristen A. Fahy[2], Scott Palo[1]

[1]University of Colorado Boulder, Boulder, Colorado
[2]Jet Propulsion Laboratory, California Institute of Technology, Pasadena, California
*Corresponding author: Jonathan Jiang (Jonathan.H.Jiang@jpl.nasa.gov)

Abstract

Clouds play a significant role in the Earth's energy balance and hydrological cycle through their effects on radiation and precipitation, and therefore are crucial for life on Earth. Earth's NexT-generation ICE mission (ENTICE) is proposed to measure diurnally resolved global vertical profiles of cloud ice particle size, ice water content, and in-cloud humidity and temperature using multi-frequency sub-millimeter (sub-mm) microwave radiometers and a 94 GHz cloud radar from space. The scientific objective of ENTICE is to identify the important processes by which anvil clouds evolve and interact with ambient thermodynamic conditions to advance our fundamental understanding of clouds and reduce uncertainties in cloud climate feedback. Whether such an objective could be achieved depends on the orbital sampling characteristics of the mission. In this study, ENTICE sampling statistics are simulated using five different scanning methods in a 400 km altitude precession orbit with an inclination of 65°: nadir, forward pointing, side scanning, and conical scanning for the radiometers, and nadir pointing for the radar. Using the GEOS-5 Nature Run produced at 7-km and 30-min resolution, sampling statistics with respect to cloud types and local hours with enhancement from radar are calculated for ENTICE. The wide swath of ENTICE radiometers by conical and side scanning methods ensures ample high cloud samples gathered by ENTICE over its two-year mission for different types of clouds with sufficient sampling over the diurnal cycles. Sampling differences between radar and radiometers at nadir demonstrate that the combination of radar and radiometers will allow for measurements of cloud vertical profiles. Therefore, our results show that the designed orbit sampling of ENTICE is sufficient to fulfill the mission science goals.

Plain Language Summary

We present a satellite orbit sampling simulator for cloud measurements from space based on the novel design of a new satellite instrument called ENTICE, which is a combined platform of

multi-frequency passive microwave radiometers and a radar detector. In this study, the simulator is flying through a modeled atmosphere at a 400 km orbit above the surface. The cloud sampling is simulated using five different observation methods. We present results over a proposed two-year ENTICE mission for different types of clouds at different diurnal varying local times. Our results show that the designed orbit sampling of ENTICE is sufficient to fulfill the mission science goals.

1. Introduction

Ice clouds play a critical role in Earth's weather and climate. They significantly impact the global hydrological cycle [*Stubenrauch et al*., 2013] and the global energy balance [*Stephens et al.*, 2012], making them crucial for life on Earth. Weather and climate anomalies are tightly associated with the radiative heating related to ice clouds [*Albern et al.*, 2020]. Specifically, tropical anvil clouds are at the heart of large uncertainties on cloud-climate feedback [*Hartmann & Berry*, 2017]. Anvil clouds are defined as clouds with convective cores and spreading clouds at upper levels whose appearance is similar to the namesake of a blacksmith's anvil [*Hartmann,* 2016] . Competing theories exist on the formation and evolution of tropical anvil clouds, which makes anvil clouds one of the least understood aspects of current atmospheric models [*Yue et al.*, 2020] . Specifically, anvil cloud duration and coverage, as well as the processes that govern those factors are not well understood. For example, the global circulation model (GCM) simulation of high-altitude ice clouds does not currently match observational data. [*Jiang et al.*, 2012, 2021; *Li et al*., 2012; *Waliser et al.*, 2009]. Moreover, a recent review article has shown that tropical anvil clouds are one of the main sources of uncertainty in climate models [*Sherwood et al.*, 2020]. The 2017 Decadal Survey states that one of its most important science goals is to reduce the uncertainty in low and high cloud feedback by a factor of 2 [ESAS 2017]. To better understand these processes, accurate measurements on vertical structures of cloud microphysical properties and the thermodynamic background conditions are necessary, which is still lacking in the current satellite observations [*Jiang et al.* 2017, 2019].

One source of climate model uncertainty on anvil clouds stems from ice cloud particle size and fall speed parameterizations. Differences in ice cloud particle size and fall speed parameterizations result in large differences in upper tropospheric cloudiness, precipitation, diurnal cycle of convection [*Elsaesser et al.*, 2017; *Li et al.*, 2015] , and cloud radiative effects [*Hourdin et al*., 2017; *Muri et al*., 2014]. *Wang et al.* [2020] show that the uncertainties of climate sensitivity can

be reduced by a factor of 2 by reducing ice particle size uncertainty by 25%. The Goddard Institute for Space Studies (GISS) model simulated ice water content (IWC) magnitude and distribution significantly improved when a new ice particle size was incorporated based on field campaign data [*Elsaesser et al*., 2017]. Therefore, it is necessary to provide better observations of ice cloud vertical profiles.

Spaceborne instruments such as radar and radiometers have been previously used to study the properties of ice clouds due to their ability to cover large areas of Earth for long periods of time [*Wang et al.*, 2019]. The Cloud-Aerosol Lidar and Infrared Pathfinder Satellite Observation (CALIPSO) and CloudSat in NASA's A-Train satellites have led to a much more complete understanding of vertical structures in clouds and precipitation [*Stephens et al., 2018; Winker et al.*, 2010]. However, limitations in CloudSat and CALIPSO still exist, especially on measuring the vertical profiles of particle sizes and in-cloud temperature and humidity. The cloud particle size retrieved from these instruments are highly subject to prior information based on empirical relationships between IWC and temperature from a limited number of field campaigns. Various validation studies have found uncertainties more than a factor of 2 in these measurements of IWC [*Jiang et al.*, 2012; *Stein et al*., 2011; *Wu et al*., 2008]. As A-Train satellites are at the end of their lifetime [*Stephens et al.*, 2018] and the Aerosol, Cloud, and Convection, and Precipitation missions are still in planning, SmallSat and CubeSat missions will provide an ideal opportunity to fill the observational void with low cost.

Earth's NexT-generation ICE mission (ENTICE) is proposed to enhance our understanding of the radiative effects and climate feedbacks of ice cloud microphysical properties [*Jiang et al*. 2019] by providing vertical profiles of ice particle size, IWC, in-cloud humidity, and temperature. ENTICE will take advantage of low-cost multi-frequency sub-mm microwave radiometers and a 94 GHz cloud radar. To sample the diurnal cycle with near-global coverage, ENTICE proposes to fly at an approximately 400 km altitude in a 65° inclined orbit. However, simulation studies are necessary to investigate whether ENTICE will return sufficient samples to meet its scientific goals.

In this study, a satellite orbiter simulator was used to determine the number of samples of different types of ice clouds the ENTICE mission would obtain and how well diurnal cycles will be sampled. Specifically, four scanning modes of radiometers were tested in this simulation and the sampling rate of nadir-pointing radar is evaluated. The four scanning modes were nadir, forward pointing, side scanning, and conical scanning (Figure 1). These modes were chosen based on previous satellite observation methods [*Fu et al*., 2020] and evaluated based on ENTICE

sensitivity to IWC and ice water path (IWP) [*Jiang et al*. 2017, 2019] using nature runs generated by the GEOS-5 Nature Run, Ganymed Release [*Putman et al.*, 2014]. Cloud types are determined following the convention of International Satellite Cloud Climatology Project [*Rossow & Schiffer*, 1991], and IWP is used to further separate the ice cloud into different categories [Jiang et al., 2015]. Sampling statistics is determined as the frequency of ENTICE observations with respect to different cloud types and local time. Diurnal sampling rate is studied over two regions of interest: the Tropical Western Pacific (TWP) and the tropical Western Atlantic (TWA).

2. Methodology and Data

2.1. Positional Data

The first step in the simulation is to generate the positional data of all the scanning methods outlined above. This is achieved by running an analytical two-body force model simulation of the satellite as it orbits the Earth. For ENTICE, the simulation uses the orbit characteristics of the Global Precipitation Mission (GPM) orbit given in Table 1 [*Matsui et al*., 2013]. These parameters are input into Kepler's equation which is solved using a Newton's method algorithm. Then, the orbital elements are converted into an Earth Centered Inertial (ECI) Frame.

Table 1: The orbital elements of the orbit used in the simulation. This orbit is based on the GPM orbit.

Orbital Element	Value
Radius of Perigee	6771 km
Radius of Apogee	6786 km
Inclination	65°

Using the position of the satellite in the ECI Frame, the simulator finds the latitude and longitude of the satellite at different local times. It then also finds the latitude and longitude for the location each scanning method is observing. For the forward pointing scan, the software rotates the position vector forward 45° in the satellites reference frame by first converting the angle to the ECI frame and then calculating the direction cosine matrix (DCM) to rotate the ECI position vector. In this case it rotates around the satellite's normalized angular momentum vector. The simulator then finds the latitude and longitude of the rotated position vector. There exists about a minute time difference between the forward pointing and nadir scanning methods. For side scanning, depending on the time, the simulator will rotate between 0° and 55° either to the right or left. The simulation software follows the same procedure as the forward pointing scan except it

varies what the angle it rotates by depending on the time and is rotating the ECI position vector around the satellite's normalized velocity vector. This in turn generates a swath width of about 1200 km. The conical scan simply combines the two above rotations into one motion. First the simulator rotates the ECI position vector forward and then to the side depending on the time. Figure 1 provides a visual depiction of each scanning method. The side and cone scans create a swath, while the nadir and forward pointing scans do not.

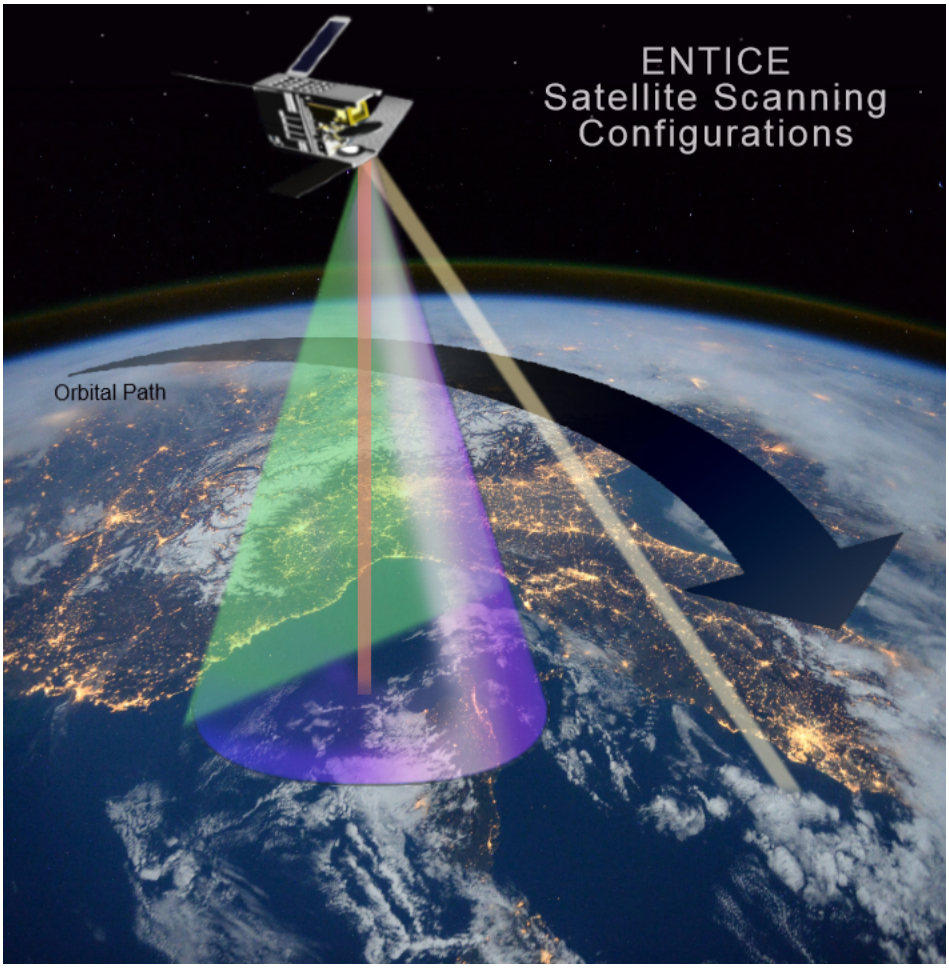

Figure 1: The four scanning methods: nadir, side, conical, and forward pointing. The nadir and forward pointing modes take observations in a straight line, while the side and conical modes cover a wide area.

In the simulation, the nadir and forward pointing scans are sampled at 10 times per second. The side and conical scans complete their swath every time the nadir and forward scans take a sample, so they sample at 100 times per second. The simulation then plots these ground tracks for reference on an equirectangular projection map of the Earth. Figure 2 shows the ground tracks of

the center of satellite fields of view from each scanning method. The side and cone modes complete one swath after the nadir and forward pointing modes complete one observation.

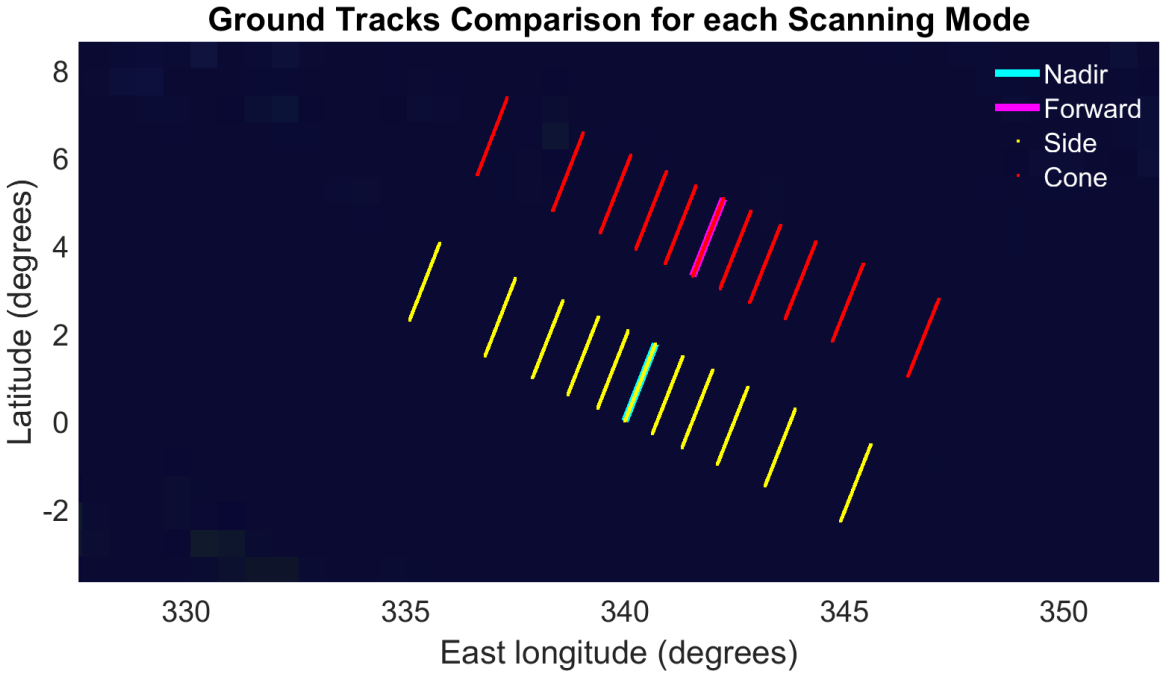

Figure 2: The initial ground tracks for each of the scanning methods. Note that in the time it takes for the nadir and forward pointing modes to make one observation, the side and conical modes have covered one swath.

2.2. Nature runs and ENTICE Instruments

The clouds and atmosphere from GEOS-5 Nature Run Ganymed Release is used in this study [*Putman et al.*, 2014]. The simulation is run at spatial and temporal resolutions of 7 km and 30 min respectively. The model atmosphere is sampled every second in the simulation. Then, each scanning method is scaled by the sampling rate discussed above, assuming that the clouds in the model atmosphere are randomly distributed. We use the cloud distribution from the model and neglect the change of clouds at the same geographical location within 30 min. For the diurnal sampling study, statistics are generated for eight 3-hr local time intervals: 0000, 0300, 0600, 0900, 1200, 1500, 1800, and 2100. For simulated observations made at high scan angles, the IWC values from multiple model grid boxes along the path of observation are used.

Four cloud path scanning methods are simulated for radiometers. The radar is only simulated on the nadir scanning method similar to CloudSat [*Heymsfield et al*., 2014] . To account for the sensitivity of radiometers used in ENTICE [*Jiang et al*. 2017, 2019], the pressure level of the first cloud layer in a column with IWC values above the threshold of 1×10^{-3} g/m^3 is recorded as

cloud top and occurrence of clouds detected by radiometers. These thresholds are between the detection limit of CALIPSO and CloudSat [*Heymsfield et al.*, 2014], which are consistent with the sensitivity of the ENTICE instrument. Extremely small IWC values below 1×10^{-8} kg/kg produced by GEOS-5 Nature Run was discarded from this analysis.

First the sampling by ISCCP cloud types is investigated. High altitude clouds are defined as any clouds above 412.5 hPa. Medium altitude clouds are defined as any cloud above 675 hPa and below 412.5 hPa. Low altitude clouds are any clouds below 675hPa. A clear sky is a column with no clouds (i.e., IWP < 1×10^{-8} kg/kg).

The radar instrument records all pressure levels of clouds in a column with IWC above a certain threshold. The radar threshold is determined using the formula shown in equation 1 [*Hong et al.,* 2008],

$$IWC = 0.0765 Z_e^{0.5414} \quad (1)$$

For this simulation we have assumed that minimum detection threshold for the radar is –20 dBz [*Heymsfield et al*., 2003], which corresponds to an IWC value of 6.3221×10^{-3}g/m^3. This is in line with the ENTICE radar instrument design.

2.3. Diurnal Cycles

The variation of sampling frequency with respect to local time is investigated for two regions of interest: TWP region (330° E to 350° E in longitude and 12° N to 12° S in latitude), and TWA (82° E to 117° E in longitude and 10° N to 30° N in latitude). These two regions were selected due to the presence of high-altitude clouds [*Brogniez & Kirstetter*, 2020; *Hartmann & Berry*, 2017]. In addition, the TWA has a significant impact on the weather and climate of the United States. Different ice cloud types represented by IWP values are analyzed.

3. Results

Figure 3 shows the map of ground tracks produced by each of the scanning methods over 24 hours. With one day of observations, the side and conical scans provide near-global coverage. It also confirms the simulation is accurately reproducing the different scanning methods. This is part of the first step in generating the positional data as described in the methodology and data section. The orbit used in this simulation is the GPM satellite orbit and was chosen as the inclination of the satellite which would help the instruments study the impact of diurnal cycles on ice cloud formation, duration, and coverage. Other satellite orbits such as Earthcare, do not provide

appropriate coverage of local times to study diurnal cycles. The inclination is too high and puts the satellite in a sun synchronous orbit [*Illingworth et al*., 2015], causing the satellite to pass over the area of interest at the same local time each day. Orbits like the international space station (ISS) on the other hand, do not provide enough spatial coverage of Earth. The inclination of the ISS is 52° [*Thirsk et al*., 2009], which is much lower than GPM's. The GPM orbit allows for a compromise between these two extremes. On top of that, the side and conical scanning modes lead to a much higher coverage of Earth on a shorter time scale. By sweeping a swath, the satellite can cover more ground than if it just had a nadir or forward pointing sensor.

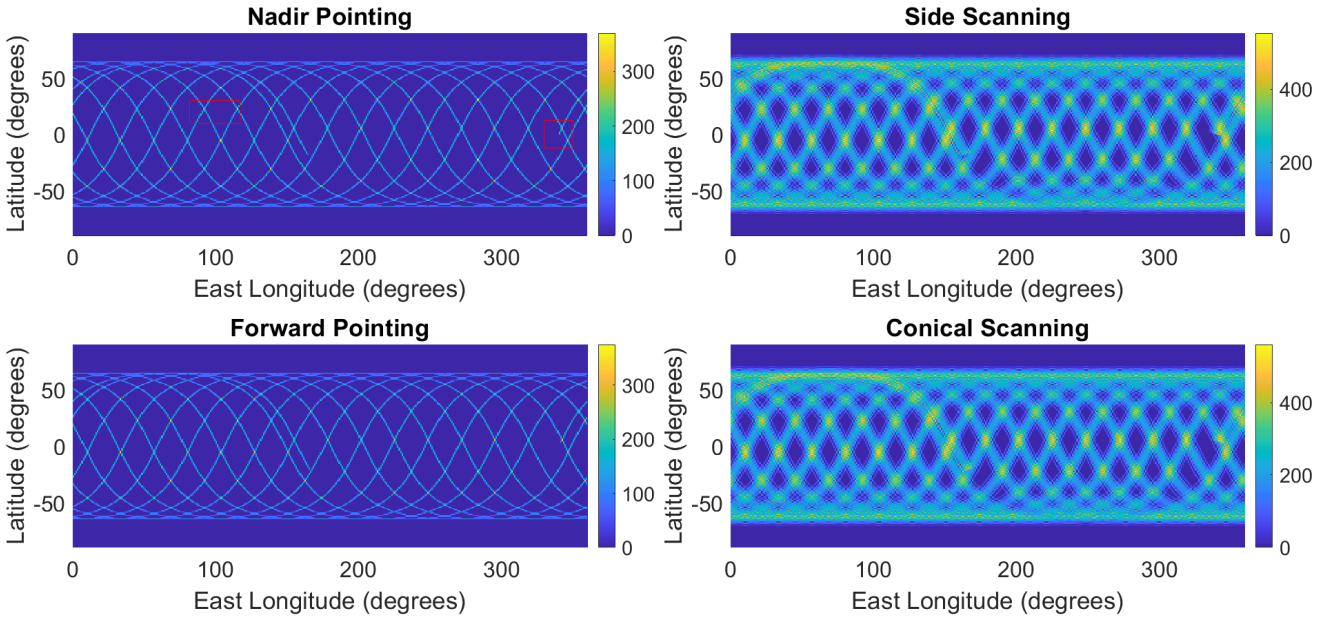

Figure 3: The ground tracks density plot for each scanning mode. The side and conical scanning modes cover a much larger area due to the large swath width. The green box around the TWP is the area of interest for the study of diurnal cycles

To illustrate the sampling of vertical profiles, Figure 4 shows a curtain plot for a short section of 250 seconds under the nadir scan mode for both radiometers and radar. The contours show the cloud fields simulated by the nature run (i.e., the truth data). The red and green symbols show the cloud altitudes measured by radiometer and radar, respectively. As discussed previously, radiometers have higher sensitivity to column integrated cloud properties and limited sensitivity to vertical profiles. Therefore, only the cloud top that reach the threshold of radiometer sensitivity is recorded. For radar, all vertical layers that are above the –20dBz detection threshold are recorded. *Jiang et al.* [2019] have shown by combining information from both radar and

radiometers, vertical profiles of cloud microphysical properties with high accuracy and vertical resolution could be achieved.

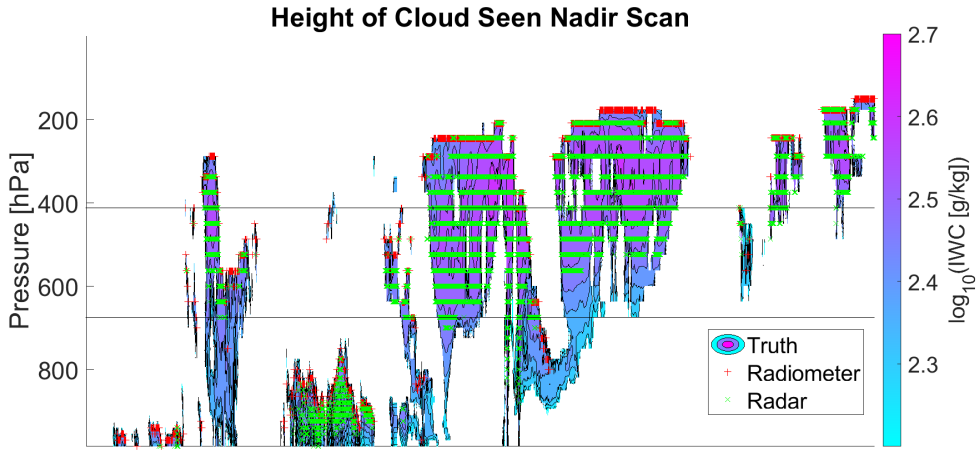

Figure 4: A curtain plot showing where the nadir radiometer and radar instruments pick up different clouds. Each instrument has different strengths for studying different aspects of high clouds.

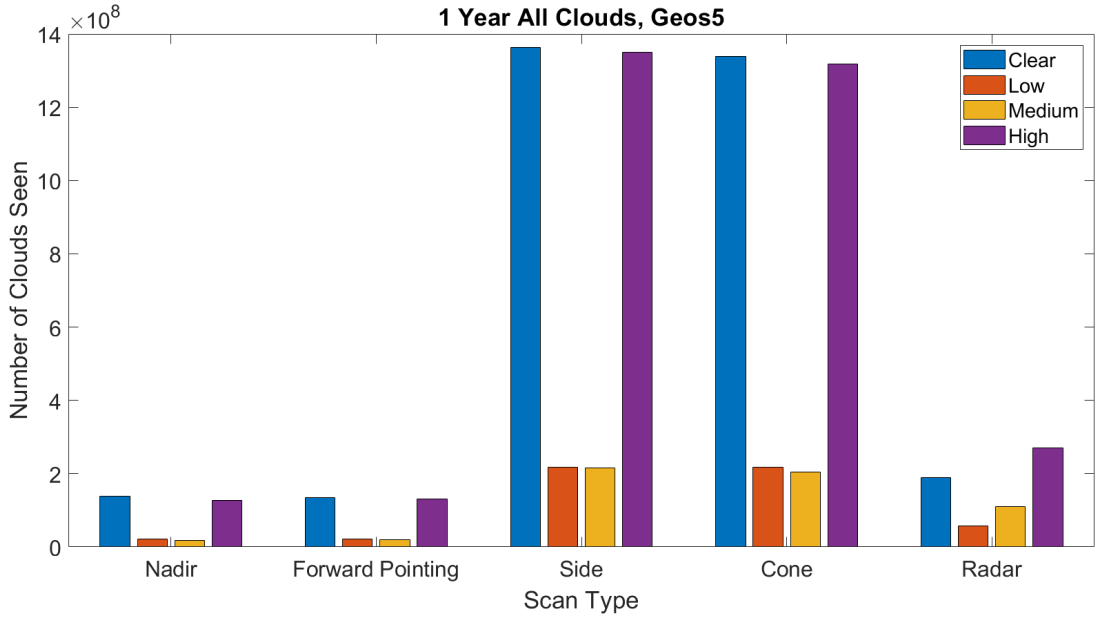

Figure 5: The number of clouds seen by each scanning method.

Figure 5 compares the total counts of observations for different cloud types using various scanning methods over an observational operation period of 1 year. The conical and side scans return much larger sample sizes on high clouds than the other scanning methods. More importantly, Figure 5 shows that ENTICE with a 2-year mission time would provide sufficient samples for different types of clouds.

Focusing on high altitude ice cloud only, Figure 6 shows the seasonal variation of samplings seen by the radar and nadir viewing radiometer over 1 year. With just one month of data, nadir observations provide ice cloud samples on a 10^7 order of magnitude.

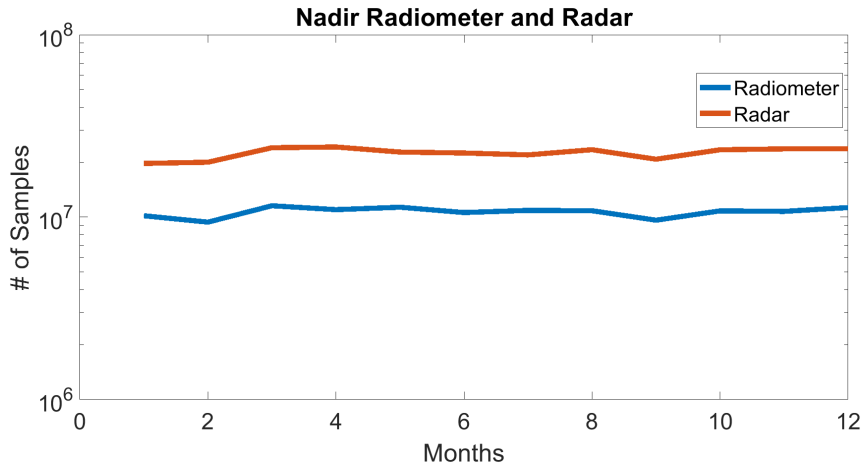

Figure 6: The difference in high-altitude ice clouds seen by the radar and radiometer.

Figure 7 shows the number of high clouds seen by each radiometer scanning method over the course of 1 year. There is no significant difference between the cone and side scan or between the nadir and forward scan.

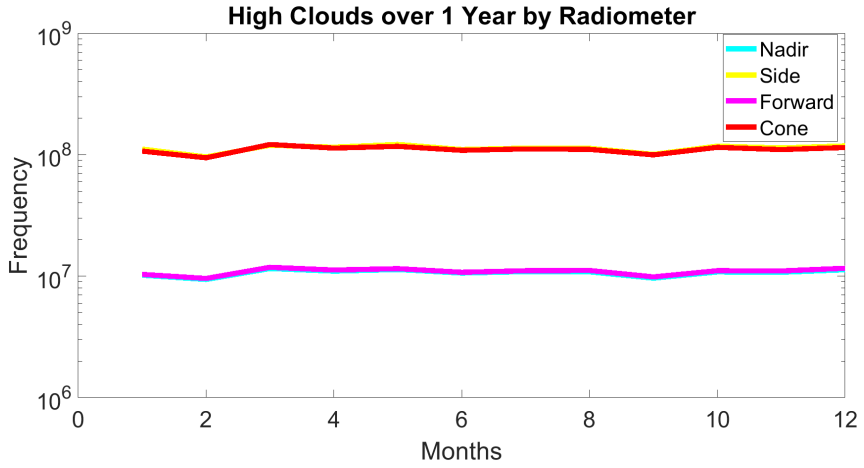

Figure 7: the number of high clouds recorded by each scanning method over 24 hours. Due to their high frequency, the side and cone methods return significantly more high clouds.

Figures 8 and 9 show ENTICE sample size for ice clouds with different ranges of IWP values in the two different regions TWA and TWP respectively. These regions were chosen not only for the large amount of high clouds present [*Brogniez & Kirstetter*, 2020; *Hartmann & Berry*, 2017], but also because the TWA has a significant pattern of moderate deep convective core occurrence and the TWP is known for its frequently occurring mesoscale convective systems [*Houze et all*].

Four IWP bins are used here: 10^{-2} to 1 g/m^2, 1 to 10 g/m^2, 10 to 100 g/m^2, and > 100 g/m^2. IWP values less than 0.01 were discarded from this analysis and the results are grouped based on the local time of the observation using 3-hour intervals. The revisit rate was 9.5 hours on average over 1 month. It varied between 11.5 and 1.5 hours. With one month of observations, large number of samples are obtained over the full diurnal cycle for both regions. Therefore, sufficient observations for different types of ice clouds will be obtained by ENTICE over the 2-year mission, which allows researchers to study the effect of diurnal cycles of ice clouds.

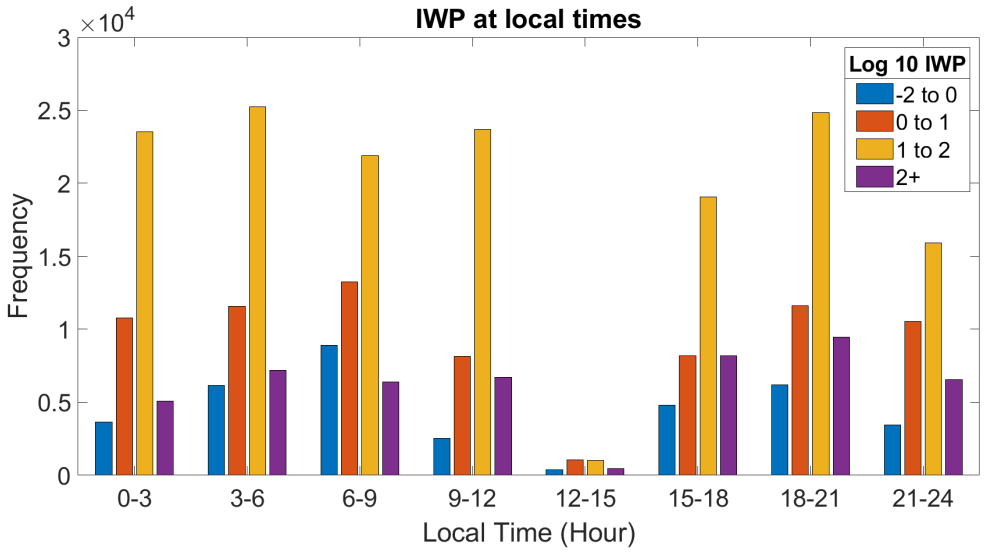

Figure 8: The IWP values recorded by the satellite simulation over 31 days over the TWA region. The minimum number of samples between 12-15 hours is over 2800 over the course of 1 month.

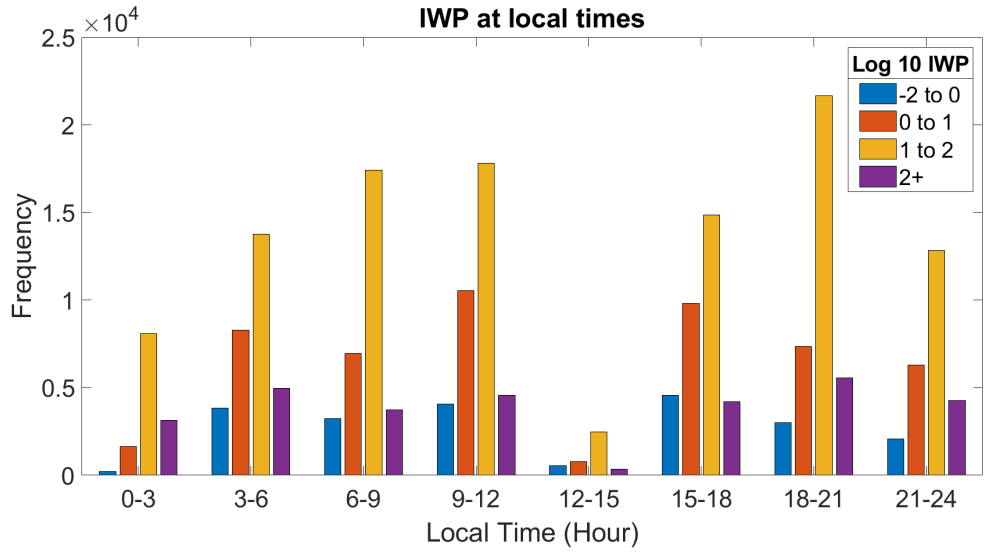

Figure 9: The IWP values recorded by the satellite simulation over 31 days over the TWP region. The minimum number of samples between 12-15 hours is over 4000 over the course of 1 month.

5 Conclusions and Discussions

A satellite orbit simulator is used in this study to investigate the sampling frequency of the proposed ENTICE mission. It used four different scanning methods for the simulated radiometer: nadir, forward pointing, side, and conical and nadir pointing for the radar. The radar instrument is able to penetrate deeper into the cloud layer than the radiometer and study cloud vertical profiles. The sampling rate for nadir and forward pointing radiometer was 10 times per second and 100 times per second for side and conical. The sampling rate for the radar was 10 times per second and the side and conical scanning methods create wide swaths that provide daily near-global coverage. These scanning methods used IWC and IWP to evaluate their effectiveness. Our results show that the number of high-altitude ice cloud samples ENTICE will return over a year-long mission is on the order of 1×10^9 with either the side scanning or conical scanning methods.

Not only that, based on the analysis of local sampling throughout the day, this data will be diurnally resolved and provide key insights into the effect diurnal cycle's role in the formation and evolution of ice clouds in the atmosphere. The IWP data gathered over a year-long simulation also demonstrate the valuable insights ENTICE will gain regarding diurnal cycles. This first of its kind data will lead to better modelling of diurnal cycles and overall better models of our atmosphere.

We have demonstrated that ENTICE will be able to gather valuable scientific information that will provide key insight into Earth's changing climate. ENTICE will provide sufficient samples to fulfill its science mission goals. By retrieving vertical profiles of ice particle size, IWC, in-cloud humidity, and temperature, ENTICE will enhance our understanding of the radiative effects and climate feedbacks of ice cloud microphysical properties. The data it gathers will undoubtedly reduce uncertainties in climate and weather modelling.

Acknowledgments, Samples, and Data

This work was conducted at the NASA-sponsored Jet Propulsion Laboratory (JPL), California Institute of Technology.

Data Statement: The data underlying this article are available in the article. The model atmosphere used in this simulation was produced by the Global Measuring and Assimilation Office at Goddard Space Flight Center (https://gmao.gsfc.nasa.gov/ global_mesoscale/7km-G5NR/). For additional questions regarding the data sharing, please contact the corresponding author at Jonathan.H.Jiang@jpl.nasa.gov.

References

Albern, N., Voigt, A., Thompson, D. W. J., & Pinto, J. G. (2020). The Role of Tropical, Midlatitude, and Polar Cloud-Radiative Changes for the Midlatitude Circulation Response to Global Warming. *Journal of Climate*, *33*(18), 7927–7943. https://doi.org/10.1175/JCLI-D-20-0073.1

Brogniez, H., & Kirstetter, P.-E. (2020). Coupling of Clouds and Tropospheric Relative Humidity in the Tropical Western Atlantic: Insights From Multisatellite Observations. *Geophysical Research Letters*, *47*(7), e2020GL087466. https://doi.org/10.1029/2020GL087466

ESAS 2017: National Academies of Sciences, Engineering, and Medicine (2017). Thriving on Our Changing Planet: A Decadal Strategy for Earth Observation from Space. Washington, DC: The National Academies Press. https://doi.org.10.17226/24938.

Elsaesser, G. S., Genio, A. D. D., Jiang, J. H., & Lier-Walqui, M. van. (2017). An Improved Convective Ice Parameterization for the NASA GISS Global Climate Model and Impacts on Cloud Ice Simulation. *Journal of Climate*, *30*(1), 317–336. https://doi.org/10.1175/JCLI-D-16-0346.1

Hartmann, D. L. (2016). Tropical anvil clouds and climate sensitivity. *Proceedings of the National Academy of Sciences*, *113*(32), 8897. https://doi.org/10.1073/pnas.1610455113

Hartmann, D. L., & Berry, S. E. (2017). The balanced radiative effect of tropical anvil clouds. *Journal of Geophysical Research: Atmospheres*, *122*(9), 5003–5020. https://doi.org/10.1002/2017JD026460

Heymsfield, A., Winker, D., Avery, M., Vaughan, M., Diskin, G., Deng, M., et al. (2014). Relationships between Ice Water Content and Volume Extinction Coefficient from In Situ Observations for Temperatures from 0° to −86°C: Implications for Spaceborne Lidar Retrievals. *Journal of Applied Meteorology and Climatology*, *53*(2), 479–505. https://doi.org/10.1175/JAMC-D-13-087.1

Heymsfield, A. J., Matrosov, S., & Baum, B. (2003). Ice Water Path–Optical Depth Relationships for Cirrus and Deep Stratiform Ice Cloud Layers. *Journal of Applied Meteorology and Climatology*, *42*(10), 1369–1390. https://doi.org/10.1175/1520-0450(2003)042<1369:IWPDRF>2.0.CO;2

Hong, G., Yang, P., Baum, B. A., & Heymsfield, A. J. (2008). Relationship between ice water content and equivalent radar reflectivity for clouds consisting of nonspherical ice particles. *Journal of Geophysical Research: Atmospheres*, *113*(D20). https://doi.org/10.1029/2008JD009890

Hourdin, F., Mauritsen, T., Gettelman, A., Golaz, J.-C., Balaji, V., Duan, Q., et al. (2017). The Art and Science of Climate Model Tuning. *Bulletin of the American Meteorological Society*, *98*(3), 589–602. https://doi.org/10.1175/BAMS-D-15-00135.1

Houze, R. A., Rasmussen, K. L., Zuluaga, M. D., & Brodzik, S. R. (2015). The variable nature of convection in the tropics and subtropics: A legacy of 16 years of the Tropical Rainfall Measuring Mission satellite. *Reviews of Geophysics (Washington, D.C. : 1985)*, *53*(3), 994–1021. https://doi.org/10.1002/2015RG000488

Illingworth, A. J., Barker, H. W., Beljaars, A., Ceccaldi, M., Chepfer, H., Clerbaux, N., et al. (2015). The EarthCARE Satellite: The Next Step Forward in Global Measurements of Clouds, Aerosols, Precipitation, and Radiation. *Bulletin of the American Meteorological Society*, *96*(8), 1311–1332. https://doi.org/10.1175/BAMS-D-12-00227.1

Jiang, J. H., Su, H., Zhai, C., Perun, V. S., Del Genio, A., Nazarenko, L. S., et al. (2012). Evaluation of cloud and water vapor simulations in CMIP5 climate models using NASA "A-

Train" satellite observations. *Journal of Geophysical Research: Atmospheres*, *117*(D14). https://doi.org/10.1029/2011JD017237.
Jiang, J.H., H. Su, L. Wu, C. Zhai, K. Schiro, Improvements in cloud and water vapor simulations over the tropical oceans in CMIP6 compared to CMIP5, Earth and Space Science, doi:10.1002/ 2021EA001520, 2021.
Jiang, J. H., Su, H., Zhai, C., Shen, T. J., Wu, T., Zhang, J., et al. (2015). Evaluating the Diurnal Cycle of Upper-Tropospheric Ice Clouds in Climate Models Using SMILES Observations. *Journal of the Atmospheric Sciences*, *72*(3), 1022–1044. https://doi.org/10.1175/JAS-D-14-0124.1
Jiang, J.H., et al., A Simulation of Ice Cloud Particle Size, Humidity and Temperature Measurements from the TWICE CubeSat, Earth and Space Science, 4, doi:10.1002/ 2017EA000296, 2017.
Jiang, J.H., Q. Yue, H. Su, P. Kangaslahti, et al., Simulation of remote sensing of clouds and humidity from space using a combined platform of radar and multi-frequency microwave radiometers, Earth and Space Science, Vol. 6, Issue 7., doi:10.1002/ 2017EA000296, 2019.
Li, J.-L. F., Waliser, D. E., Chen, W.-T., Guan, B., Kubar, T., Stephens, G., et al. (2012). An observationally based evaluation of cloud ice water in CMIP3 and CMIP5 GCMs and contemporary reanalyses using contemporary satellite data. *Journal of Geophysical Research: Atmospheres*, *117*(D16). https://doi.org/10.1029/2012JD017640
Li, Y., Thompson, D. W. J., & Bony, S. (2015). The Influence of Atmospheric Cloud Radiative Effects on the Large-Scale Atmospheric Circulation. *Journal of Climate*, *28*(18), 7263–7278. https://doi.org/10.1175/JCLI-D-14-00825.1
Matsui, T., Iguchi, T., Li, X., Han, M., Tao, W.-K., Petersen, W., et al. (2013). GPM Satellite Simulator over Ground Validation Sites. *Bulletin of the American Meteorological Society*, *94*(11), 1653–1660. https://doi.org/10.1175/BAMS-D-12-00160.1
Muri, H., Kristjánsson, J. E., Storelvmo, T., & Pfeffer, M. A. (2014). The climatic effects of modifying cirrus clouds in a climate engineering framework. *Journal of Geophysical Research: Atmospheres*, *119*(7), 4174–4191. https://doi.org/10.1002/2013JD021063
Putman, W. M., Silva, A. M. da, Ott, L. E., & Darmenov, A. (2014). Model Configuration for the 7-km GEOS-5 Nature Run, Ganymed Release. [Non-hydrostatic 7 km Global Mesoscale Simulation].
Rossow, W. B., & Schiffer, R. A. (1991). ISCCP Cloud Data Products. *Bulletin of the American Meteorological Society*, *72*(1), 2–20. https://doi.org/10.1175/1520-0477(1991)072<0002:ICDP>2.0.CO;2
Sherwood, S. C., Webb, M. J., Annan, J. D., Armour, K. C., Forster, P. M., Hargreaves, J. C., et al. (2020). An Assessment of Earth's Climate Sensitivity Using Multiple Lines of Evidence. *Reviews of Geophysics*, *58*(4), e2019RG000678. https://doi.org/10.1029/2019RG000678
Stein, T. H. M., Delanoë, J., & Hogan, R. J. (2011). A Comparison among Four Different Retrieval Methods for Ice-Cloud Properties Using Data from CloudSat, CALIPSO, and MODIS. *Journal of Applied Meteorology and Climatology*, *50*(9), 1952–1969. https://doi.org/10.1175/2011JAMC2646.1
Stephens, G., Winker, D., Pelon, J., Trepte, C., Vane, D., Yuhas, C., et al. (2018). CloudSat and CALIPSO within the A-Train: Ten Years of Actively Observing the Earth System. *Bulletin of the American Meteorological Society*, *99*(3), 569–581. https://doi.org/10.1175/BAMS-D-16-0324.1

Stephens, G. L., Li, J., Wild, M., Clayson, C. A., Loeb, N., Kato, S., et al. (2012). An update on Earth's energy balance in light of the latest global observations. *Nature Geoscience*, *5*(10), 691–696. https://doi.org/10.1038/ngeo1580

Stubenrauch, C. J., Rossow, W. B., Kinne, S., Ackerman, S., Cesana, G., Chepfer, H., et al. (2013). Assessment of Global Cloud Datasets from Satellites: Project and Database Initiated by the GEWEX Radiation Panel. *Bulletin of the American Meteorological Society*, *94*(7), 1031–1049. https://doi.org/10.1175/BAMS-D-12-00117.1

Thirsk, R., Kuipers, A., Mukai, C., & Williams, D. (2009). The space-flight environment: the International Space Station and beyond. *CMAJ : Canadian Medical Association Journal*, *180*(12), 1216–1220. https://doi.org/10.1503/cmaj.081125

Waliser, D. E., Li, J.-L. F., Woods, C. P., Austin, R. T., Bacmeister, J., Chern, J., et al. (2009). Cloud ice: A climate model challenge with signs and expectations of progress. *Journal of Geophysical Research: Atmospheres*, *114*(D8). https://doi.org/10.1029/2008JD010015

Wang, C., Platnick, S., Fauchez, T., Meyer, K., Zhang, Z., Iwabuchi, H., & Kahn, B. H. (2019). An Assessment of the Impacts of Cloud Vertical Heterogeneity on Global Ice Cloud Data Records From Passive Satellite Retrievals. *Journal of Geophysical Research: Atmospheres*, *124*(3), 1578–1595. https://doi.org/10.1029/2018JD029681

Wang, Y., H. Su, J. H. Jiang, F. Xu, Y. Yung "Impact of Cloud Ice Particle Size Uncertainty in A Climate Model and Implications for Future Satellite Missions", J. Geophys. Res. 125, 6 (2020)

Winker, D. M., Pelon, J., Coakley, J. A., Ackerman, S. A., Charlson, R. J., Colarco, P. R., et al. (2010). The CALIPSO Mission: A Global 3D View of Aerosols and Clouds. *Bulletin of the American Meteorological Society*, *91*(9), 1211–1230. https://doi.org/10.1175/2010BAMS3009.1

Wu, D. L., Jiang, J. H., Read, W. G., Austin, R. T., Davis, C. P., Lambert, A., et al. (2008). Validation of the Aura MLS cloud ice water content measurements. *Journal of Geophysical Research: Atmospheres*, *113*(D15). https://doi.org/10.1029/2007JD008931

Yue, Q., Jiang, J. H., Heymsfield, A., Liou, K.-N., Gu, Y., & Sinha, A. (2020). Combining In Situ and Satellite Observations to Understand the Vertical Structure of Tropical Anvil Cloud Microphysical Properties During the TC4 Experiment. *Earth and Space Science*, *7*(4), e2020EA001147. https://doi.org/10.1029/2020EA001147